3rd Specialty Conference on Disaster Prevention and Mitigation
3e Conférence spécialisée sur la prévention et la mitigation des désastres naturels

Montréal, Québec
May 29 to June 1, 2013 / *29 mai au 1 juin 2013*

Unrestrained Thermal Deformations of Concrete Elements Exposed to Fire

S.F. El-Fitiany and M.A. Youssef
Department of Civil and Environmental Engineering, Western University, London, ON

Abstract: Fire impacts Reinforced Concrete (RC) members by raising the temperature of the concrete mass. This rise in temperature dramatically reduces the mechanical properties of concrete and steel and induces new strains, thermal and transient creep. As a result, heated RC members undergo considerable thermal deformations during fire events. This paper presents a comprehensive parametric study to evaluate the unrestrained thermal deformation parameters, curvature and axial strain, for rectangular RC sections during ASTM-E119 fire exposure. These parameters describe the section's free thermal expansion at different fire durations. The proposed expressions can be used by engineers to estimate the restraint effect in indeterminate RC structures exposed to fire.

Keywords: Concrete; Fire; Sectional analysis; Fire performance, Thermal deformation, Restraint effect.

1. Introduction

Fire initiates when combustible materials ignite. Then, it spreads horizontally and/or vertically depending on the compartment boundaries (Lie et al. 1992). A temperature gradient is generated through exposed RC elements. These elevated temperatures reduce the element's stiffness and produce thermal deformations (El-Fitiany and Youssef 2012). A simplified sectional analysis method to estimate the thermal deformations of RC elements during fire exposure was developed and validated by El-Fitiany and Youssef (2009). Although this method simplifies analysis of RC structures at elevated temperatures, it requires knowledge of heat transfer principles and ability to account for effect of elevated temperatures on stiffness and deformations.

In this paper, a number of RC rectangular sections with different cross-section dimension, reinforcement configuration, and material properties are analyzed during the standard ASTM-E119 fire exposure. The unrestrained thermal deformation for each cross-section is evaluated. Results of the parametric study are used to provide designers with simplified expressions for the expected thermal deformations of RC beams subjected to ASTM-E119 fire exposure. These expressions allow estimating the induced secondary axial forces and/or moments due to fire heating in indeterminate structures.

2. Prediction of the Thermal Deformation using Sectional Analysis Method

Fire temperature drastically decreases concrete and steel mechanical properties and induces thermal and transient strains. Total concrete strain at elevated temperatures (ε) is composed of three terms: unrestrained thermal strain (ε_{th}), instantaneous stress related strain (ε_c), and transient creep strain (ε_{tr}). Fire performance of RC beams can be predicted by summing those strain components as given by Equation 1.

[1] $\varepsilon = \varepsilon_{th} + \varepsilon_c + \varepsilon_{tr}$

A sectional analysis approach suitable for the analysis of rectangular RC beams at elevated temperatures was proposed by El-Fitiany and Youssef (2009). Figure 1a shows the used fiber model. The beam is assumed to be exposed to fire from three sides. Thermal deformations can be obtained by applying the following main steps:

- At specific fire duration, a heat transfer analysis is conducted and the temperature distribution through the cross section is predicted. The cross-section is then divided into horizontal layers and two average temperatures, T_σ and T_{th}, are assigned to each layer, Figure 1b. T_σ and T_{th} are calculated to represent the average layer strength and the average layer temperature, respectively.

- The nonlinear thermal strain (ε_{th}) distribution, shown in Figure 1g, is calculated using T_{th}. The thermal strain of steel bars is calculated based on the concrete temperature at their location.

- ε_{th} is then converted to an equivalent linear thermal strain ($\overline{\varepsilon_{th}}$) by considering self equilibrium of internal thermal forces in concrete and steel layers, Figure 1. The linear distribution is characterized by the unrestrained thermal axial strain, ε_i, and curvature, ψ_i. Figure 1f shows the differences between the equivalent linear and nonlinear thermal strains, which represent the self-induced thermal strains (ε_{st}). These strains are assigned as initial strains for the concrete and steel layers to model the corresponding self-induced thermal stresses at a given point of the fire temperature-time curve. The total strain (ε) can be described as follows

[2] $\varepsilon = \overline{\varepsilon_{th}} + \varepsilon_{st} + \varepsilon_c + \varepsilon_{tr}$

- Youssef and Moftah (2007) proposed constitutive stress-strain relationships for concrete and steel, which implicitly accounts for the transient creep ε_{tr}. The instantaneous stress-related strain (ε_c), self-induced thermal strain (ε_{st}), and the transient strain (ε_{tr}) terms are lumped in a mechanical strain term (ε_{cT}). ε_{ct} is then added to $\overline{\varepsilon_{th}}$ to calculate total effective strain ε. Equation 2 can be rewritten as follows

[3] $\varepsilon = \overline{\varepsilon_{th}} + \varepsilon_{cT}$

- Using the concrete and steel constitutive relationships that is based on T_σ, the corresponding stress is calculated. By considering the equilibrium of the stresses of all the layers, the corresponding moment can be calculated. The behavior of the analyzed cross-section is presented by moment (M)–curvature (ψ) and the axial load (P)-axial strain (ε) diagrams.

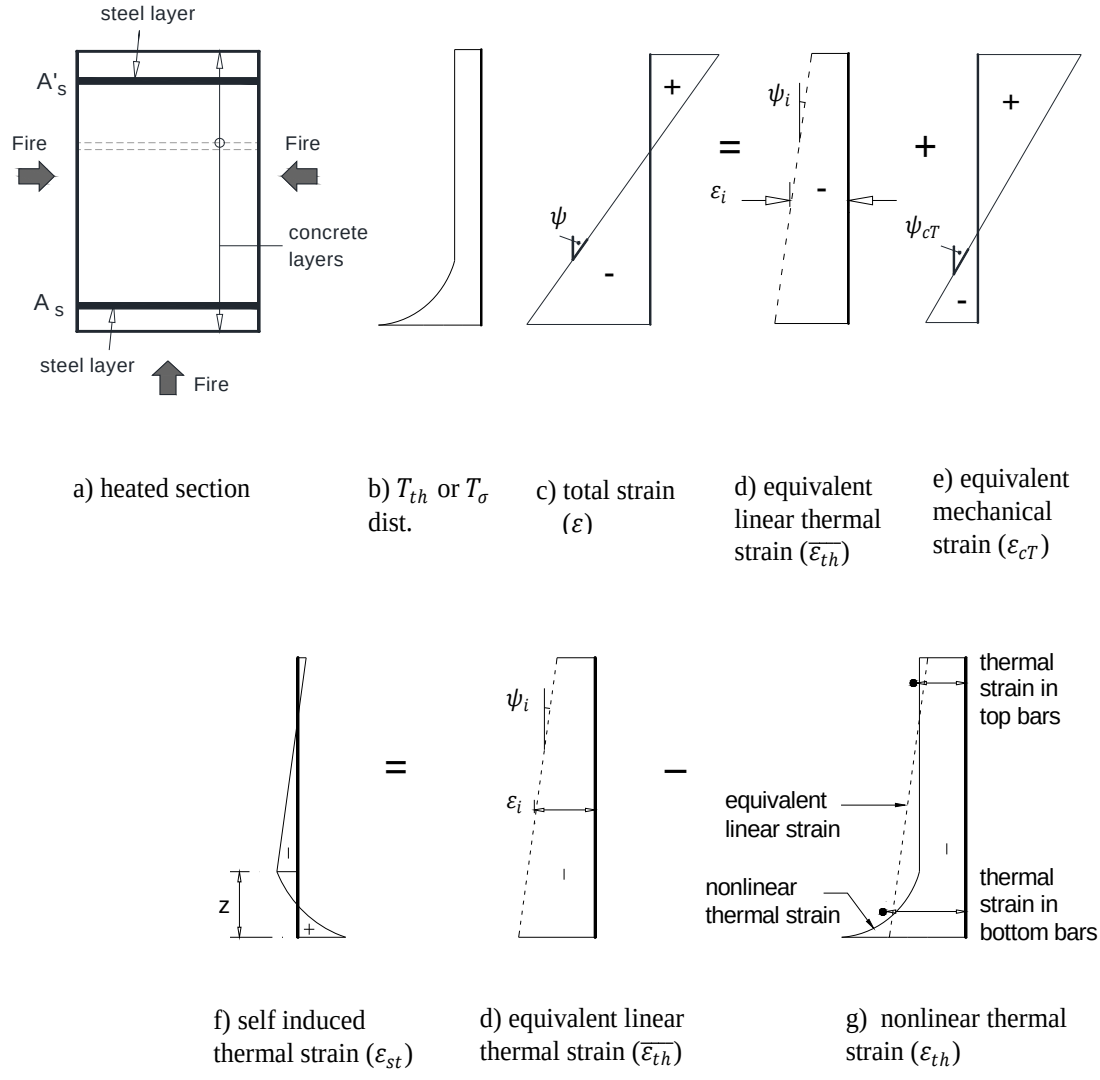

Figure 1: Sectional analysis approach for RC sections exposed to fire

3. Moment-Curvature Relationships of Fire-Heated Sections

In this section, characteristics of M–ψ relationships are discussed. Figure 2 shows schematics for the M–ψ curves for RC sections subjected to sagging and hogging moments. The end point on the curve defines the nominal moment capacity (M_n) that corresponds to the curvature capacity of the analyzed cross-section. Considering an assumed fire duration, it can be stated that the effect of thermal strain on the M–ψ relationship is constant regardless of the load level. This constant effect describes the free thermal expansion of the unloaded concrete element. It results in shifting the M–ψ diagram by a value ψ_i that can be predicted by calculating the nonlinear thermal strain distribution and converting it to an equivalent linear distribution. The $M-\psi$ diagram includes the effects of material degradation, transient creep strain (ε_{tr}), and self induced thermal strain (ε_{st}). The total curvature (ψ) is the sum of the unrestrained thermal curvature (ψ_i) and the mechanical curvature (ψ_{cT}) and can be expressed by Eq. 4.

[4] $\psi = \psi_i + \psi_{cT}$

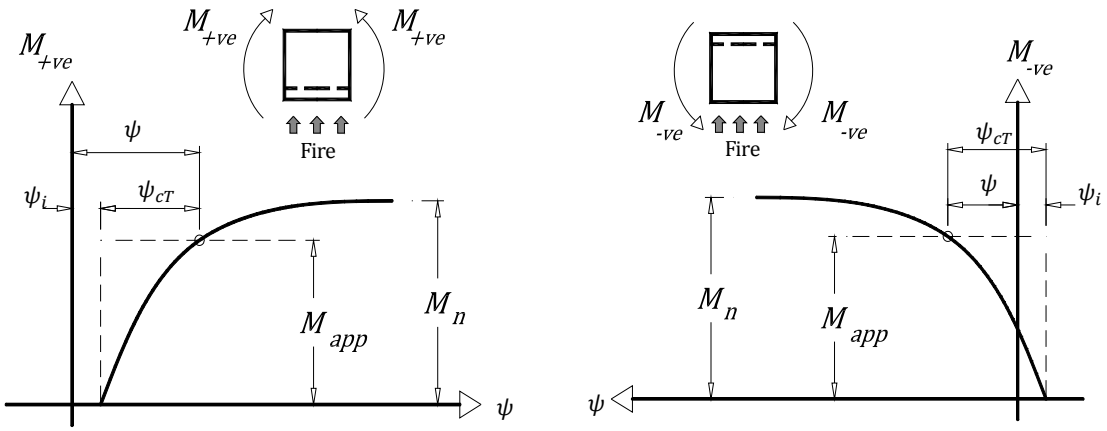

a) sagging moments (M_{+ve}) b) hogging moments (M_{-ve})

Figure 2: (M)–(ψ) diagrams for RC beams during fire

As shown in Figure 2, heating RC beams from the bottom face and the two sides cause the lower concrete fibers to thermally expand more than the upper concrete fibers and results in ψ_i. The acting moment induces a mechanical curvature (ψ_{cT}), which is either added to ψ_i or subtracted from it.

Similar observations can be stated about the axial force-axial strain relationship. The total axial strain (ε) is the sum of the unrestrained thermal strain (ε_i) and the mechanical strain (ε_{cT}).

4. Evaluation of Thermal Parameters

In this section, the effects of different geometric and material factors on the thermal deformation parameters $\psi_i$and $\varepsilon_i$are discussed using a comprehensive parametric study. The study aims at providing structural engineers with simple expressions to evaluate these parameters without the need for heat transfer and sectional analysis calculations.

Table 1 summarizes the properties of the analyzed beams. All the beams have rectangular cross-section and are subjected to ASTM-E119 standard fire exposure from three sides as shown in Figure 3. The considered parameters are width (b), height (h), concrete compressive strength (f'_c), number of tensile steel layers ($n = 1, 2$), aggregate type (Agg), compression reinforcement ratio ($\rho' = 0.06\% - 0.65\%$), and tensile reinforcement ratio ($\rho = 0.5\% - 2.5\%$). The standard reinforcement layout, shown Figure 3, is assumed in this study. The parametric study is limited to siliceous and carbonate concretes with compressive strength (f'_c) ranging between 20 and 50 MPa . The fire duration (t) ranges from 0.0 to 2.5 hr.

Table 1: Parametric study cases

Beam #	b (mm)	h (mm)	f'_c (MPa)	n	Agg	$\rho'\%$ (A_g)	$\rho\,\%$ (A_g)
B1	300	500	30	1	siliceous	0.13	0.5
B2							1.0
B3				2			1.5
B4							2.5
B5	300	700		1	siliceous	0.10	0.5
B6				2			1.0
B7							1.5
B8							2.5
B9	400	700		2	siliceous	0.07	1.0
B10							2.5
B11	500	700		2	siliceous	0.06	1.0
B12							2.5
B13	300	300		1	siliceous	0.22	1.5
D1	300	500	20	1	siliceous	0.13	0.5
D2							1.0
D3				2			1.5
D4							2.5
D5	300	700	40	1	siliceous	0.10	0.5
D6				2			1.0
D7							1.5
D8							2.5
D9	400	700	50	2	siliceous	0.07	1.0
D10							2.5
D11	500	700	50	2	siliceous	0.06	1.0
D12							2.5
I1	300	500	30	1	siliceous	0.13	0.5
I2					carbonate	0.13	1.0
I4	300	700	40	2	siliceous	0.25	1.0
I5						0.45	
I6						0.65	
I7	300	700	40	2	carbonate	0.10	1.5
I8	300	700	40	2	siliceous	0.10	1.0
I9						0.10	
I10	400	700	50	2	siliceous	0.15	2.5

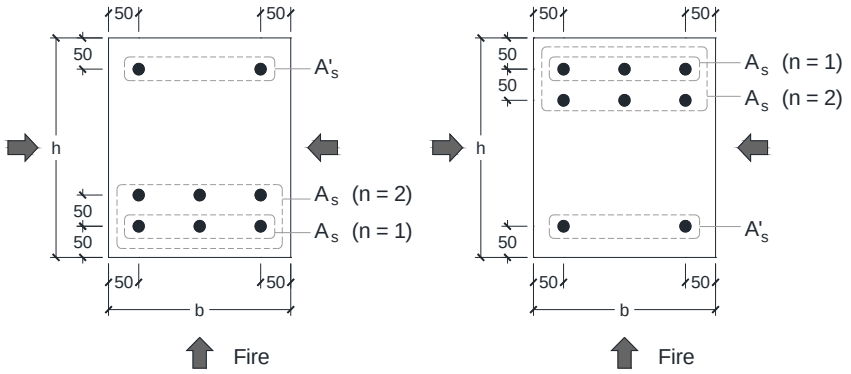

a) sagging moments (M_{+ve}) b) hogging moments (M_{-ve})

Figure 3: Typical cross-sections for the parametric study beams
(Dimensions in mm)

4.1 Analysis and discussion

A heat transfer analysis is conducted and the nonlinear thermal distribution is converted to a uniform thermal distribution. The values of the unrestrained thermal curvature ψ_i and axial strain ε_i are estimated at each time step up to $2.5\ \mathrm{hr}$. Figures 4 to 8 show the variation of ε_i and ψ_i for the studied sections considering both positive and negative bending. Observations about these figures are given below.

4.1.1 Factors having negligible effect

The effect of the tensile reinforcement ratio ρ and concrete compressive strength f'_c on ε_i and ψ_i is found to be negligible as shown in Figure 4.

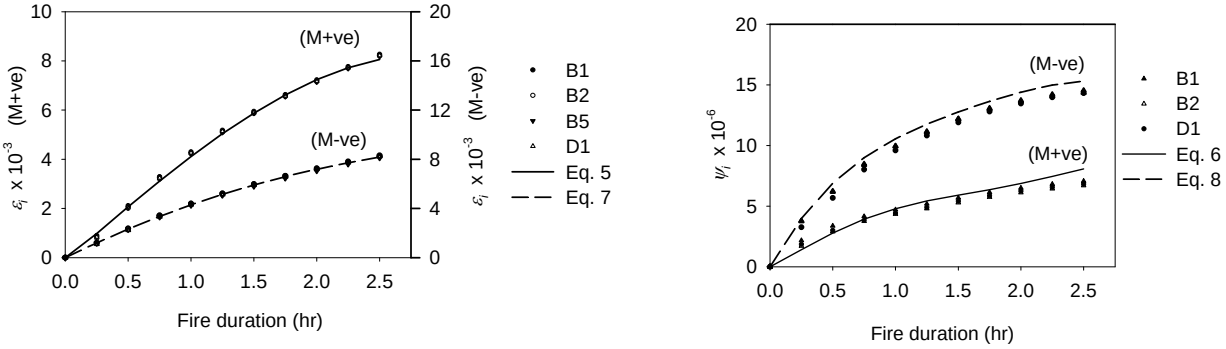

Figure 4: Effect of ρ and f'_c on ε_i and ψ_i
(Curvature in $1/mm$)

4.1.2 Effect of section dimensions (b, h)

Increasing the aspect ratio $\mathrm{b/h}$ decreases the thermal expansion of the concrete mass due to the lower concrete mass temperature, Figure 5. ψ_i is significantly increased for wide cross-sections due to the low thermal conductivity of concrete that results in substantial temperature difference between the lower and top concrete masses.

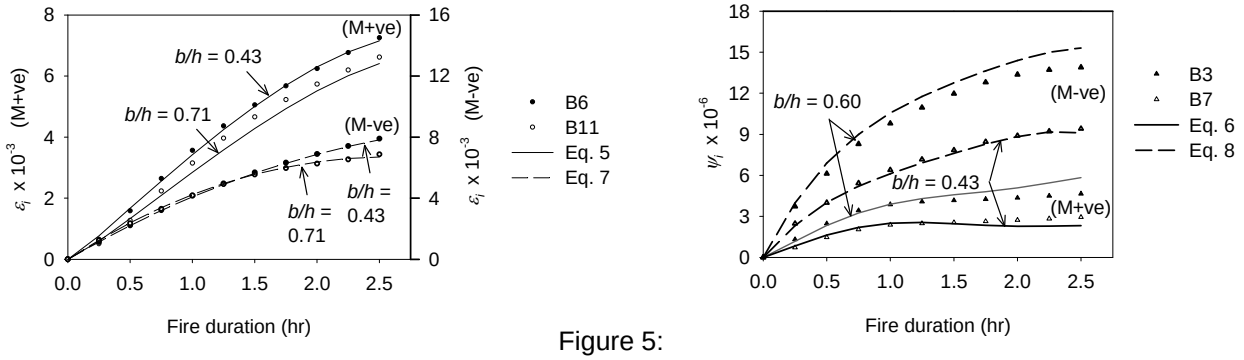

Figure 5:
Figure 6: Effect of cross-section dimensions on ε_i and ψ_i
(Curvature in $1/mm$)

4.1.3 Effect of Reinforcement configuration

Figure 6 indicates that distributing the steel bars on two layers instead of one layer has a minor effect on the ε_i and ψ_i. For the cases of two reinforcement layers, the lower temperature in the heated steel bars limits the thermal expansion of the surrounding concrete. Increasing the compression reinforcement ratio ρ' has a minor effect on ε_i. However, it reduces ψ_i slightly for the case of negative moments and considerably for the case of positive moments. Compression reinforcing bars are heated from two sides for the case of negative moment, which dramatically reduces their yield strength and consequently do not control the concrete expansion anymore.

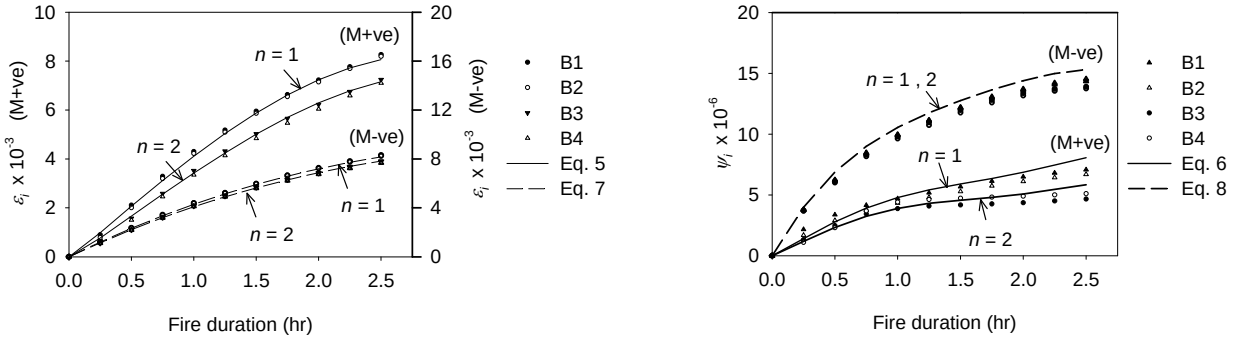

Figure 7: Effect of number of tensile reinforcement layers n on ε_i and ψ_i
(Curvature in $1/mm$)

4.1.4 Effect of aggregate type

The effect of aggregate type (Agg) is shown in Figure 7. Concrete with carbonate aggregate has less thermal expansion than concrete with siliceous aggregate (Lie et al. 1992, Youssef and Moftah 2007). The effect of the aggregate type on the curvature is negligible for the case of sagging (positive) moment as the expansion of the lower concrete is highly dependent on the bottom steel reinforcement expansion rather than the expansion of the concrete itself. On the other hand, the location of tensile steel bars at the top of cross-sections, i.e. case of negative moment, makes the thermal expansion of the lower concrete mass more predominant as its expansion is not controlled by substantial amount of steel bars.

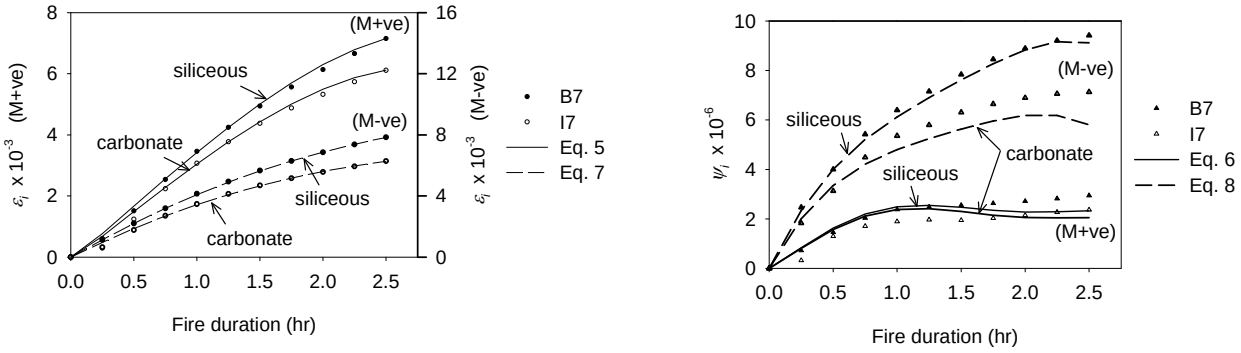

Figure 8: Effect of number of aggregate type Agg on ε_i and ψ_i
(Curvature in $1/mm$)

4.2 Proposed expressions for the unrestrained thermal parameters ε_i and ψ_i

The predicted values of ε_i and ψ_i, based on the parametric study, are analyzed using a multiple regression analysis technique (Wonnacott and Thomas 1985). A number of expressions are proposed to predict the unrestrained thermal parameters ε_i and ψ_i for rectangular RC sections subjected to ASTM-E119 fire exposure up to 2.5 hr. The proposed equations are only valid for the cross-sections covered in the parametric study. Figure 8 shows the relationship between the analytical predictions, using the sectional analysis, and the values obtained by applying the proposed expressions.

For cross-sections subjected to positive (sagging) moments, a typical cross-section is shown in Figure 3a, ε_i and ψ_i can be predicted using Eqs. (5) and (6), respectively. Predictions of the proposed equations are plotted in Figures 4 to 7 and indicated by solid lines. Structural engineers can use the proposed equations to represent the thermal expansion when modeling RC beams using available structural analysis tools.

[5] $$\varepsilon_i = -1.275 \times 10^{-4} - 1.725 \times 10^{-4} \times t^3 + (-5.365 + 2.186 \times n - 0.269 \times Agg + 9.291 \times 10^{-3} \times b) \times t^2 \times 10^{-4} + (64.986 - 9.068 \times n - 3.483 \times Agg - 3.809 \times 10^{-2} \times b) \times t \times 10^{-4}$$

[6] $$\psi_i = -1.994 \times 10^{-8} - 1.023 \times 10^{-9} \times b \times t^5 + (4.072 \times 10^{-2} \times b + 8.683) \times t^4 \times 10^{-7} - (38.884 + 2.025 \times 10^{-2} \times b) \times t^3 \times 10^{-7} + (46.997 - 8.670 \times 10^{-2} \times b) \times t^2 \times 10^{-7} + (68.490 - 7.108 \times 10^{-2} \times h + 0.103 \times b - 5.968 \times \rho') \times t \times 10^{-7} + (11.131 \times n \times Agg - 23.381 \times Agg - 8.897 \times n) \times t \times 10^{-7}$$

Where,

ε_i is the unrestrained thermal axial strain at fire duration $t \geq 0.25$

ψ_i is the unrestrained thermal curvature at fire duration $t \geq 0.25$

t is the ASTM-E119 fire duration in hrs (t ≥ 0.25 hr)

Agg is a factor to account for the aggregate type (0.0 for siliceous concrete and 1.0 for carbonate concrete)

n is the number of tensile reinforcement layers

b is the cross-section width in mm

h is the cross-section height in mm

ρ' percentage of compression reinforcement relative to $(b \times d)$

d is the effective depth of tensile reinforcement in mm

For cross-sections subjected to hogging (negative) moments, a typical cross-section is shown in Figure 3b, Eqs. (7) and (8) can be used to estimate the unrestrained thermal axial strain ε_i and curvature ψ_i, respectively. Predictions of the proposed Eqs. (7) and (8) are plotted on Figures 4 to 7 and indicated by dashed lines.

[7] $$\varepsilon_i = -3.934 \times 10^{-5} + 3.502 \times 10^{-5} \times t^3 + (-2.642 + 0.452 \times n + 0.277 \times Agg - 2.004 \times 10^{-2} \times b) \times t^2 \times 10^{-4} + (45.372 - 2.513 \times n - 6.909 \times Agg + 2.758 \times 10^{-2} \times b) \times t \times 10^{-4}$$

[8] $$\psi_i = -9.604 \times 10^{-8} - 6.698 \times 10^{-7} \times t^4 + (62.166 - 3.430 \times 10^{-2} \times h) \times t^3 \times 10^{-7} + (-214.634 + 0.185 \times h) \times t^2 \times 10^{-7} + (348.066 - 0.372 \times h + 9.388 \times 10^{-2} \times b - 13.252 \times Agg) \times t \times 10^{-7}$$

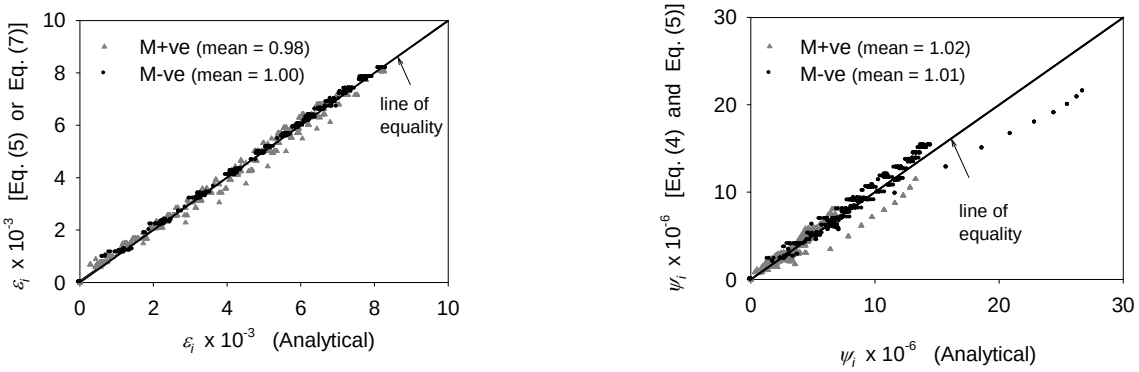

Figure 9: Regression analysis of ε_i and ψ_i
(Curvature in $1/mm$)

5. Summary and Conclusions

The application of sectional analysis to analyze RC sections exposed to fire is summarized in this paper. This method allows obtaining the moment-curvature and axial force-axial strain relationships. Examining these relationships, it was concluded that the unrestrained thermal strains and curvatures do not depend on the loading level.

A comprehensive parametric study is then conducted to investigate the effect of different material, reinforcement configuration, and geometric factors on the unrestrained thermal parameters ε_i and ψ_i. For simplicity, the parametric study is limited to rectangular RC beams subjected to $2.5\ \mathrm{hr}$ ASTM-E119 standard fire exposure and typical reinforcement configurations. Based on the results of the parametric study, a number of expressions are proposed to predict ε_i *and* ψ_i for sections subjected to both sagging (positive) and hogging (negative) moments. Designers can use these expressions to quickly predict the free thermal expansion of RC beams during fire exposure.

6. Acknowledgments

This research was funded by the Natural Sciences and Engineering Research Council of Canada (NSERC).

7. References

Lie, T.T., ed., "Structural Fire Protection," *ASCE Manuals and Reports on Engineering Practice*, no. 78, New York, NY, 1992, 241 pp.

El-Fitiany, S., Youssef, M.A. 2009, "Assessing the flexural and axial behaviour of reinforced concrete members at elevated temperatures using sectional analysis", *Fire Safety Journal*, vol. 44, no. 5, pp. 691-703.

El-Fitiany S.F. and Youssef M.A. (in press), “Simplified method to analyze continuous RC beams during fire exposure", *ACI Struct. J.*, accepted Oct 2012

Youssef, M.A. and Moftah, M., "General stress-strain relationship for concrete at elevated temperatures," *Engineering Structures*, vol. 29, no. 10, 2007, pp. 2618-2634.

Kodur, V.K.R., and Dwaikat, M., "Performance-based fire safety design of reinforced concrete beams," *Journal of Fire Protection Engineering*, vol. 17, no. 4, 2007, pp. 293-320.

El-Fitiany, S.F., and Youssef, M.A., “Stress Block Parameters for Reinforced Concrete Beams During Fire Events,” *Innovations in Fire Design of Concrete Structures*, ACI SP-279, 2011, pp. 1-39.

Wonnacott, R.J. and Wonnacott, T.H., 1985 (fourth edition), “Introductory statistics”, *New York: John Wiley & Sons*.